

# Ultra Compact Laser Based Projectors and Imagers

Harald Schenk, Thilo Sandner, Christian Drabe, Michael Scholles,  
Klaus Frommhagen, Christian Gerwig, and Hubert Lakner

Fraunhofer Institute for Photonic Microsystems (FhG-IPMS), Maria-Reiche-Str. 2,  
01109 Dresden, Germany

**Abstract.** 2D micro scanning mirrors are presented which make use of a degressive spring allowing to achieve an optical scan range of up to  $112^\circ \times 84^\circ$ , optically. The scanning mirrors are deployed for highly miniaturized monochrome and full color projectors as well as for laser imagers. The projectors allow for projection with VGA resolution at 50 Hz frame rate. The laser imager supports full color SVGA resolution at 30 Hz frame rate. Both, the projector and the imager are based on a single 2D scanner chip and thus could be combined in a single ultra compact system for simultaneous imaging and projection with high depth of focus.

**Keywords:** scanner, projection, imager, MEMS, micro scanning mirror.

## 1 Introduction

Visualization is and probably will also be in the future the most important method to transfer information from a computer to the human user/operator. To control the computer the keyboard is beginning to be replaced e. g. by touch screens and systems for gesture recognition. Latter one is possible w/o any sensors attached to the user/operator if the gestures are recorded by an imager and classified respectively interpreted by the computer.

Laser based projection and imaging offer the advantage of large depth of focus. This allows us to omit any adjustable focusing optics and thus to miniaturize the system. At the same time projected images are sharp even on surfaces with large topologies. Correspondingly, sharp images can be taken from objects with large topologies or with strongly varying distance to the imager.

The paper is focusing on projectors and imagers based on 2D micro scanning mirrors. The principle set-ups of both systems are very similar, as shown in Fig. 1. A combination of projection and imaging in one system using a single 2D scanning mirror is possible.

The paper starts with an introduction to the working principle and design of the 2D micro scanning mirror including the integrated sensor for position read-out. After that a monochrome and a full color projector are presented. In the next section a laser imager is presented which is deployed in an endoscope tip. Finally, a short outlook is given which further developments of the scanning mirror are targeted to meet future resolution requirements.

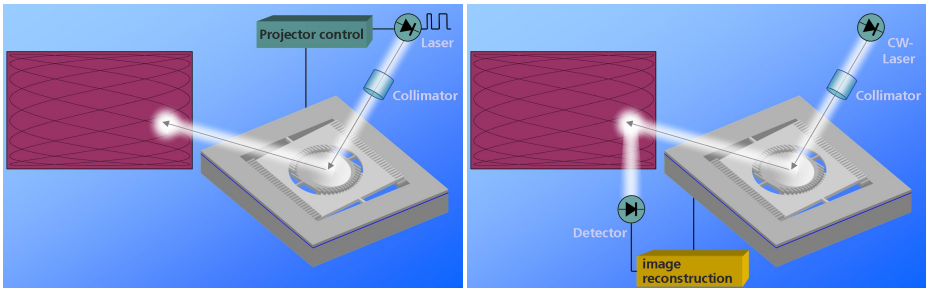


Fig. 1. Left: Schematic set-up of a laser projector. Right: Schematic set-up of a laser imager.

## 2 2D Micro Scanning Mirrors

The electrostatic driven 2D micro scanning mirrors are fabricated in a CMOS compatible micromachining process. The mirror plate as well as all mechanical elements are made from a single crystalline silicon layer with a thickness of 30  $\mu\text{m}$ , typically. Figure 2 compares an actual fabricated chip with a schematic chip drawing. The highly doped silicon layer serves as electrical conductor. By means of filled insulation trenches the respective electrical paths are defined allowing us to excite and control the oscillation of the mirror plate and of the movable frame independently. On the actual device the path of the filled insulation trenches is designed as symmetric as possible with respect to both oscillation axes. For electrical connection the insulation path is only shortly interrupted at the respective location.

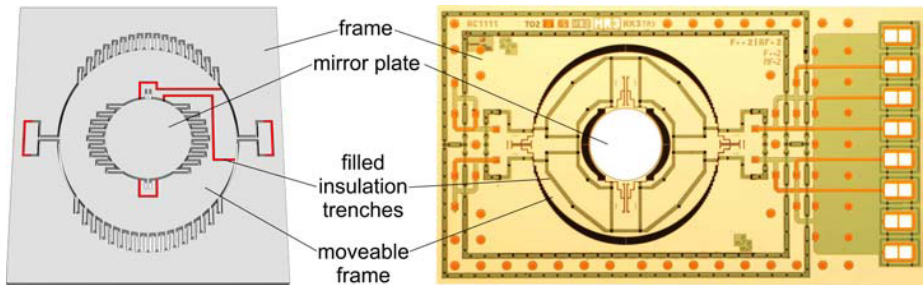
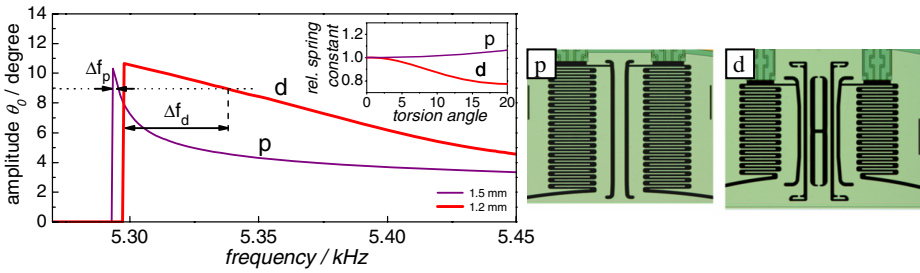


Fig. 2. Schematic drawing and micrograph of an actual chip

Applying a train of voltage pulses of suitable frequency between the respective comb electrode pairs an oscillation of the mirror plate and the movable frame, respectively is observed. Since the driving torque depends on the capacity change and thus on the deflection angle we are dealing with a parametric oscillator. The most important part of a typical response curve of the mirror plate is shown in Figure 3, left. Shape and properties of the movable frames' response curve do correspond. The curve denoted by "p" is typical for a torsion spring which constant is independent of the torsion angle or shows a slight increase with increasing angle (compare inset of



**Fig. 3.** Left: Typical response curve of a mirror plate suspended by progressive “p”, respectively degressive “d” springs. The actual mirror plates have a diameter of 1.5 mm and 1.2 mm, respectively. Right: The two micrographs detail the design of the respective springs. A small part of the circular mirror plate can be seen at the bottom of both graphs.

Fig. 3). Typically, such behavior is observed for a straight torsion bar as shown in the micrograph denoted by “p” in Fig. 3.

At a given maximum driving voltage there is a bandwidth  $\Delta f$  which allows us to meet a given oscillation amplitude. Exemplary, in Fig. 3 an oscillation amplitude of  $9^\circ$  was chosen. Obviously, the bandwidth  $\Delta f_p$  of the progressive spring is very small.

For the operation of a 2D scanner for projection or imaging the frequency ratio of the mirror plate and the movable frame influences resolution and can not be chosen arbitrarily. With frequency tolerances induced by the fabrication process and frequency variations at changing environmental conditions there is a need to have a bandwidth  $\Delta f$  as large as possible. A possible solution is the use of springs showing decreasing spring constant with increasing torsion angle. The characteristic curve of such a degressive “d” spring is shown in the inset of Fig. 3, left. This behavior is achieved by combining several suspensions near to the torsion axis (compare micrograph denoted “d” in Fig. 3). The combined effect of torque and bending moments at deflection results in the degressive character up to a certain torsion angle. The net effect on the response curve is clearly visible in Fig 3, left. The bandwidth  $\Delta f_d$  of the degressive spring is significantly larger than that of the progressive spring. Therefore, with maximum driving voltage a much broader range of frequency mismatch can be adjusted.

As the torsion springs are made from single crystalline silicon the mechanical properties do not degrade over time. Thus, open loop operation is possible. In this case the oscillation amplitude is determined by the excitation frequency and the driving voltage. However, as already indicated above, change of environmental conditions affects the response curve and the phase. For this reason closed-loop control of the oscillation amplitude and phase determination is required. In the case of projection this allows us to correctly synchronize the video data. Similar, for imaging it allows to correctly reconstruct the image. Especially because of the sinusoidal time-dependence of the deflection angle this has to be done with high accuracy.

Read-out of phase and amplitude can be done optically by directing the beam of a laser or an LED to the mirror which scans the beam over an array of photo detectors or a position sensitive device (PSD). A higher level of miniaturization is achieved with an integrated position sensor. In the following, an integrated piezo-resistive sensor is detailed which has been implemented as a volume transducer. This approach

enables to fabricate the sensor without any additional layers for the sensor like e. g. polycrystalline silicon on the surface. Instead, the p+ doped single crystalline 30  $\mu\text{m}$  thick layer itself is used. Basically, the mechanical and the mechano-electrical transducers are combined. The principle is illustrated in Figure 4.

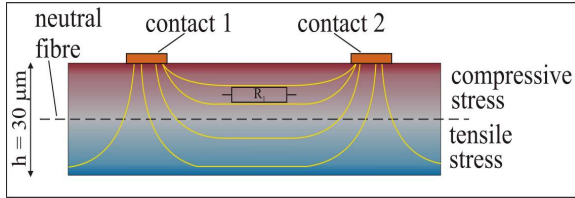


**Fig. 4.** Left: Illustration of the volume transducers' principle

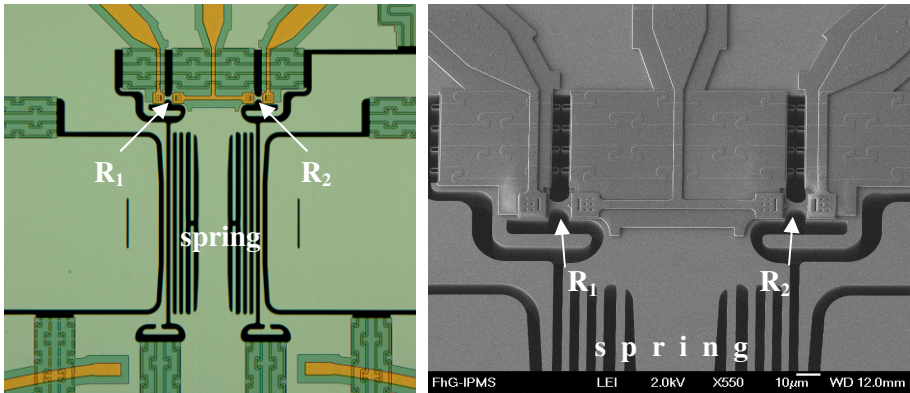


**Fig. 5.** Micrograph and SEM of a spring suspension with transducer elements forming the resistors  $R_1$  and  $R_2$ . The spring is highly degressive.

The transducer is contacted by surface contacts, close to each other. This results in a significant asymmetric distribution of the electrical field with respect to the neutral fibre. At bending of the structure the resistance change is dominated by the deformation in the upper half where the electrical field lines are much denser than in the lower part.

Figure 5 shows a detail of the spring suspension of a fabricated scanning mirror with two transducer elements forming the resistors  $R_1$  and  $R_2$ . The transducers are mechanically connected to the spring. The spring consists of a central torsion beam and  $2 \times 4$  parallel beams near to the torsion axes. This design results in a highly degressive spring. When the spring experiences torsion the two transducer elements are bent. Consequently, one resistance increases while the other one decreases. With the help of a half-Wheatstone gauge, the resistance change is read out. Figure 6 shows the experimental determined voltage output of the sensor from Fig. 5. The output voltage linearly depends on the scan amplitude  $\theta_0$  in a very good approximation. Sensitivity of the sensor is  $0.414 \mu\text{V}/(\text{V}^\circ)$ .

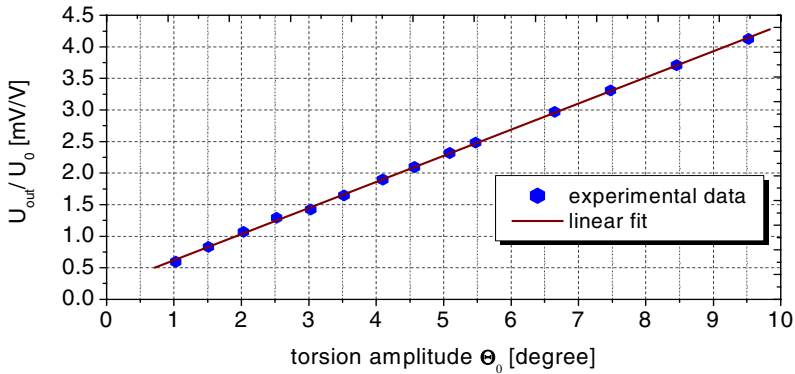


Fig. 6. Normalized output voltage of the sensor

### 3 Laser Projector

In comparison to any array based projectors like LCDs or micro mirror arrays, scanning mirror based laser projection has two distinctive advantages. First, the image is always in focus. No optics is needed to create a sharp image. Consequently, the image can even be projected sharply on non-planar surfaces. Further, one single 2D mirror chip, together with the bandwidth of the laser source and the electronic circuit, determines the resolution. Increased resolution is provided e. g. by an increase of the scan angle while in array based approaches the number of pixels has to be raised. In other words, the chip size and thus the whole size of the projector can be realized significantly smaller than in the case of any existing array based solution especially for medium and high resolution.

MEMS-scanner based projection works similar to a cathode ray tube. Instead of the electron beam a laser beam is deflected two dimensionally. However, while electrons can easily be deflected and thus fast linear scans can be performed, laser deflection requires a mechanical movable mirror. Due to the inertial moment of the mirror extremely large forces are required to perform a linear scan for the fast axis. Therefore, in general at least the fast axis is excited resonantly to make use of the power savings expressed by the quality factor (e. g. Microvisions' BiMag-Scanner 1). The projector described in the following uses a resonant driving for both axes. Consequently, the trajectory of the laser beam forms a Lissajous-pattern.

The system architecture of the laser projector is illustrated in Fig. 7. A USB interface is used to transmit the data from the PC to the electronic circuit realized by an FPGA. The PC software reads and decodes still image formats as well as audio video interleave (AVI) type video files. The data are sent continuously to the projection system. The image/video data are fed forward to two dual-ported RAMs (DPRAMs) acting as image buffer. Double buffering is used so that the DPRAMs can be large enough to store two full video frames. The two sides of the DPRAMs are connected separately to the FPGA, so that simultaneous image-write from the USB interface and image-read of the previous image for video processing is enabled.

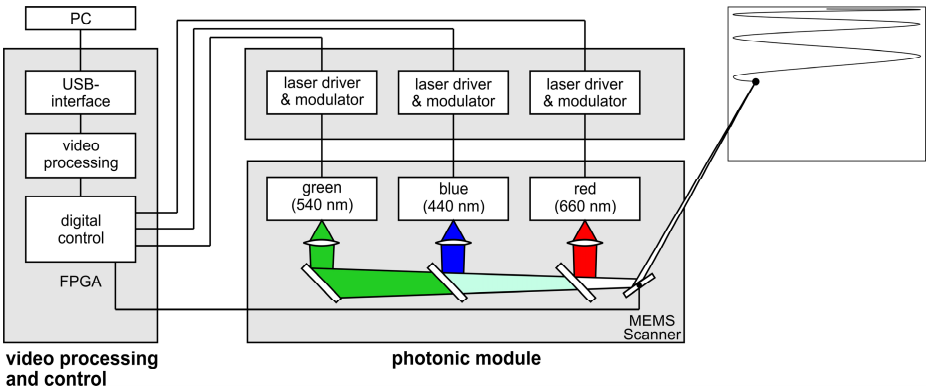


**Fig. 7.** System architecture of the laser projector

The FPGA includes the driver for the 2D MEMS scanner. For that TTL voltage pulses are generated which then are transformed to the required voltage level by MOSFETs. Based on the driving pulses and the known phase between pulse and mirror oscillation the current coordinates of the laser beam can be computed. From the image RAM the corresponding grey value is read out. The grey value is corrected with respect to the non-linear motion of the laser beam. Consequently, the laser intensity for a certain grey value at the image border (low speed of the laser spot) has to be smaller than in the middle of the image (high speed). For laser intensity modulation a digital signal with a depth of 8 bit for each color is forwarded to the laser driver / modulator.

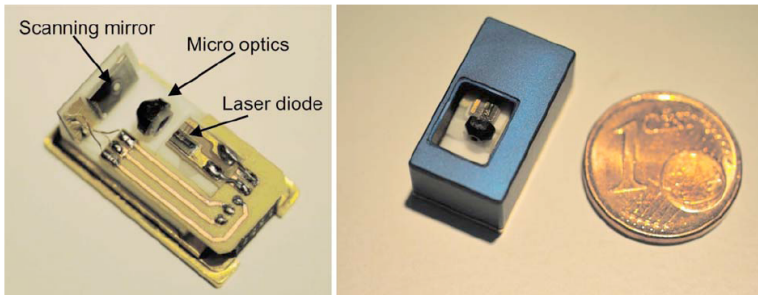


**Fig. 8.** Left: monochrome VGA projector without housing. Right: projector with housing.

The FPGA has been used to drive both, a monochrome projector which allows us to demonstrate the miniaturization potential and a full color projector which total dimensions still suffer from the fact that small RGB laser modules are not yet commercially available.

In the case of the monochrome projector a laser diode emitting at 660 nm and an optical power of 50 mW has been implemented. The frame rate is 50 Hz. Figure 8 shows the highly miniaturized VGA-projector with a dimension of 17 x 7 x 5 mm<sup>3</sup>.



**Fig. 9.** Test images of the monochrome VGA-projector

Figure 9 shows three test images demonstrating that arbitrary shapes can be projected despite the Lissajous trajectory.

For full color projection three lasers are implemented with an optical intensity of 30 mW, each. The three laser beams are combined by dichroitic filters and directed to the 2D scanning mirror. Resolution and frame rate is identical to that of the monochrome projector. Figure 10 shows the RGB projector as well as a test image.

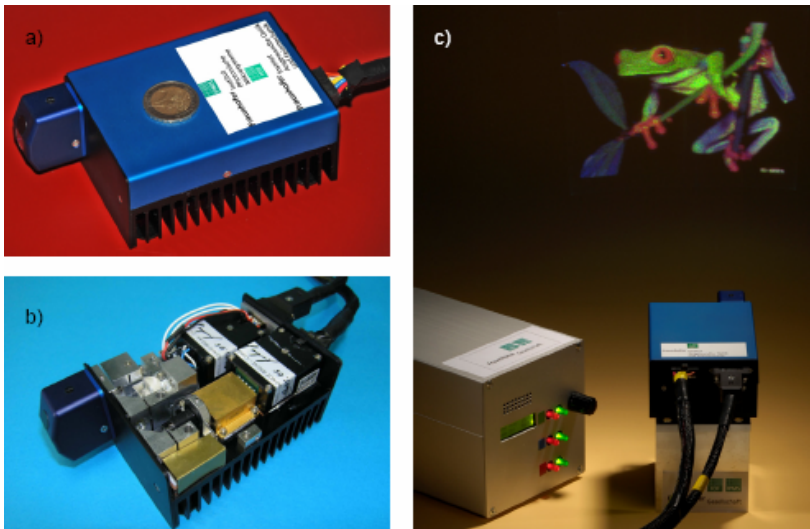


**Fig. 10.** RGB laser projector. a) housing with projection head. b) without housing: The RGB lasers are visible, c) full color image with VGA resolution and 8 bit color depth for each color.

## 4 Laser Imager

For imaging, the laser beam in principal is scanned like in the case of the projector along a Lissajous-pattern (compare Fig. 1). The laser, however, is not modulated but emits continuously, i. e. in the cw-mode. The light reflected back from the object is collected and directed to a detector. The time dependent signal of the detector is

correlated to the time-dependent deflection angle and from this, the image is reconstructed.

The system architecture of the scanned beam imaging system 2, 3 is illustrated in Figure 11. For a full color image, three lasers (RGB) are combined with dichroitic filters and focused onto a single mode glass fiber which guides the light to the 2D scanning mirror. Due to the oscillation of the micro mirror the RGB-beam is scanned across the object.

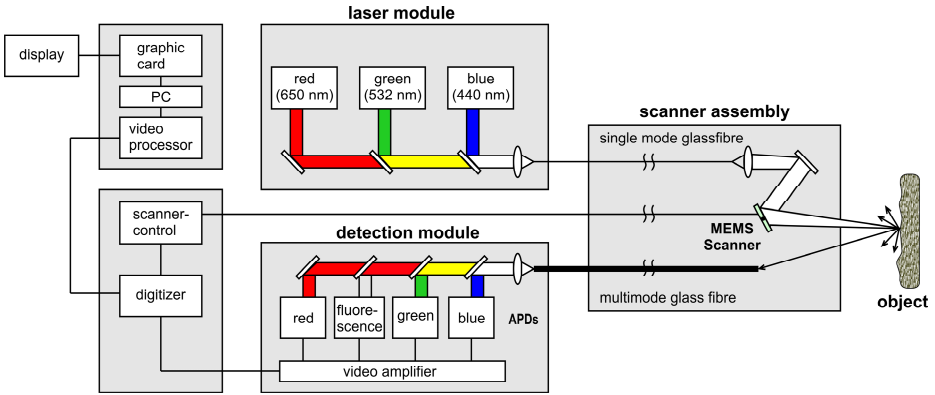


**Fig. 11.** System architecture of the laser imager (after 2)

The diffusely back reflected light is collected by several multimode fibers near to the MEMS scanner. The light is guided to the detection module where three dichroitic mirrors split the light according to the respective emission wavelength and direct it to the respective detectors. Due to the bandwidth requirements Avalanche photodiodes (APDs) are deployed which are thermoelectrically cooled to reduce Johnson noise. The laser imager offers further to detect signals at wavelengths between the excitation wavelengths or even below. In our case the system includes an additional detector for fluorescence signals.

The signal at the respective detector is amplified and digitized with a rate of 50 MHz and 12 bit resolution. From the time-dependent signal and the corresponding deflection angle of the 2D scanning mirror the image is reconstructed in real time and displayed for the user.

The system performance was demonstrated by Microvision by means of an endoscope 3. The objective was to achieve an optical scan range of  $112^\circ \times 84^\circ$  and SVGA (600 x 800) resolution at a frame rate of 30 Hz. For that a 2D scanning mirror with a frequency of 1 kHz for the slow axis and 16 kHz for the fast axis was developed and fabricated at FhG-IPMS. The high deflection angle required degressive springs. Simulation showed that a Y-shaped form provides a high operation bandwidth and allows us to keep the mechanical stress within the target range.

Figure 12a shows a photograph of the 8 mm diameter endoscope tip including the glass fibers and the 2D scanner. A picture taken through the glass dome shows the assembled scanning mirror (Figure 12b). A full color sample image with SVGA resolution at 30 Hz is shown in Figure 12c. The laser imaging inherent property of



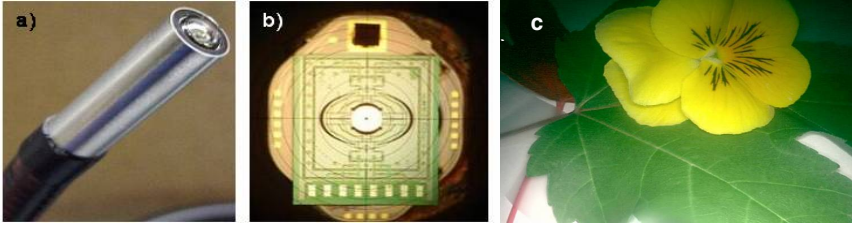


**Fig. 12.** a) Endoscope tip with a diameter of 8 mm. b) Photo through the glass dome. The 2D scanner is visible. The mirror contains a 50  $\mu\text{m}$  hole for illumination from the backside. c) sample image with SVGA resolution. (courtesy of Microvision).

very large focus depth allows to image samples with large topographies respectively at varying distance.

Note that deploying modulated laser sources instead of cw-lasers would allow us to switch between imaging and projection with a single ultra-compact device. Alternatively, imaging and projection could be done at the same time but at different wavelengths or even at the same wavelengths when using two sources.

## 5 Outlook for System Optimization

With increasing resolution the required electronic bandwidth of both, the laser projector and the laser imager is increasing. In case of the laser projector the bandwidth of the laser modulation has to be enlarged accordingly. To keep bandwidth requirements and thus system complexity low a linear scan is advantageous. For the fast axis it seems impossible to generate the required forces while keeping power consumption low. In case of the slow scanning axis, however, required forces are significantly lower. In comparison to a bi-sinusoidal scan, the bandwidth requirements for laser and electronics with the slow axis being linearly deflected and, for the sake of power saving, the fast axis being resonantly excited is lower by a factor of  $\pi/2$ .

A linear scan requires the generation of a force which allows to deflect the mirror out-of-plane in a quasistatic manner. Our approach is to permanently deflect the driving electrode comb out of the chip plane. The permanent deflection is achieved by bonding a cover wafer comprising an activation stamp to the mirror wafer as illustrated in Fig. 13.

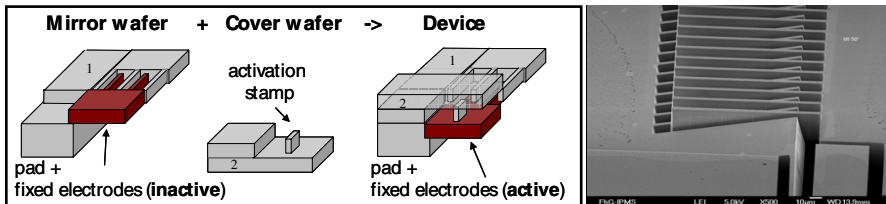


**Fig. 13.** Left: Functionalizing packaging. The stamp of the cover wafer deflects the comb permanently. Right: SEM graph of a test structure. The left comb is torsional deflected.

Preliminary simulation results show that a scan angle of up to  $\pm 10^\circ$  mechanically in the static mode can be achieved (depending on the scan/switching frequency). Experimentally, the principle was proved by test structures. An example is shown in Fig. 13, right. A more detailed description of the approach including simulation results is found in 4.

## 6 Summary and Conclusions

2D micro scanning mirrors were presented with resonant driving for both axes. Large scan angles of up to  $112^\circ \times 84^\circ$  optically are supported by deploying degressive springs for the suspension of the mirror plate and the movable frame.

An ultra compact laser projector and an ultra compact laser imager were presented. With the availability of small RGB-laser modules both systems can be further miniaturized. In principle, both systems can be combined and realized with one single 2D scanning mirror, only.

To support higher resolutions a novel approach to realize a quasistatic scanner was presented. Here, the permanent out-of-plane deflection of the driving comb for the slow axis is achieved by a functionalizing packaging.

## Acknowledgment

The authors would like to thank Dr. Andreas Bräuer from FhG-IOF for the cooperation with respect to the laser projector and Microvision for the cooperation regarding the endoscope.

## References

1. Yalcinkaya, A.D., Urey, H., Brown, D., Montague, T., Sprague, R.: Two-axis electromagnetic microscanner for high resolution displays. *J. of Microelectromechanical Systems* 15, 786–794 (2006)
2. Drabe, C., James, R., Klose, T., Wolter, A., Schenk, H., Lakner, H.: A new micro laser camera. In: *Proc. of SPIE, San Jose, USA*, vol. 6466, pp. 64660I-1–8 (2007)
3. James, R., Gibson, G., Metting, F., Davis, W., Drabe, C.: Update on MEMS-based Scanned Beam Imager. In: *Proc. of SPIE, San Jose, USA*, vol. 6466, pp. 64660J-1–11 (2007)
4. Jung, D., Kallweit, D., Sandner, T., Conrad, H., Schenk, H., Lakner, H.: Fabrication of 3D Comb Drive Microscanners by mechanically induced permanent Displacement. In: *Proc. of SPIE, San Jose, USA*, vol. 7208, pp. 72080A-1–11 (2009)